Research Article

Molecular Cancer Therapeutics

Sensitization to Radiation and Alkylating Agents by Inhibitors of Poly(ADP-ribose) Polymerase Is Enhanced in Cells Deficient in DNA Double-Strand Break Repair

Dana A. Löser[1], Atsushi Shibata[1], Akiko K. Shibata[1], Lisa J. Woodbine[1], Penny A. Jeggo[1], and Anthony J. Chalmers[1,2]

Abstract

As single agents, chemical inhibitors of poly(ADP-ribose) polymerase (PARP) are nontoxic and have clinical efficacy against BRCA1- and BRCA2-deficient tumors. PARP inhibitors also enhance the cytotoxicity of ionizing radiation and alkylating agents but will only improve clinical outcomes if tumor sensitization exceeds effects on normal tissues. It is unclear how tumor DNA repair proficiency affects the degree of sensitization. We have previously shown that the radiosensitizing effect of PARP inhibition requires DNA replication and will therefore affect rapidly proliferating tumors more than normal tissues. Because many tumors exhibit defective DNA repair, we investigated the impact of double-strand break (DSB) repair integrity on the sensitizing effects of the PARP inhibitor olaparib. Sensitization to ionizing radiation and the alkylating agent methylmethane sulfonate was enhanced in DSB repair–deficient cells. In *Artemis*$^{-/-}$ and *ATM*$^{-/-}$ mouse embryo fibroblasts, sensitization was replication dependent and associated with defective repair of replication-associated damage. Radiosensitization of *Ligase IV*$^{-/-}$ mouse embryo fibroblasts was independent of DNA replication and is explained by inhibition of "alternative" end joining. After methylmethane sulfonate treatment, PARP inhibition promoted replication-independent accumulation of DSB, repair of which required Ligase IV. Our findings predict that the sensitizing effects of PARP inhibitors will be more pronounced in rapidly dividing and/or DNA repair defective tumors than normal tissues and show their potential to enhance the therapeutic ratio achieved by conventional DNA-damaging agents. *Mol Cancer Ther; 9(6); 1775–87. ©2010 AACR.*

Introduction

The cytotoxic effects of ionizing radiation and alkylating chemotherapeutic drugs are mediated through DNA damage. Ionizing radiation induces single-stranded and double-stranded DNA breaks in an approximate ratio of 25:1 (1), whereas alkylating agents induce base damage that gives rise to single-strand breaks (SSB) and stalled replication forks. SSB induced by ionizing radiation or alkylating agents are predominantly repaired by base excision repair, whereas double-strand breaks (DSB) are repaired mainly by the nonhomologous end-joining (NHEJ) pathway (2). DSB associated with DNA replication or occurring during G_2 phase are also repaired by homologous recombination (2). Radiation-induced DSB are frequently associated with base or sugar damage, repair of which requires contributions from base excision repair proteins such as polynucleotide kinase (3). Furthermore, DSB can arise from SSB occurring in close proximity or as a consequence of DNA replication.

Because the cytotoxicity of DNA damaging agents correlates with the number of unrepaired DSB (4), inhibition of DNA repair represents a mechanism by which the therapeutic effects of these agents might by enhanced. Such enhancement must be tumor specific if outcomes are to be improved. Whereas cancer cells are typically characterized by aberrant cell cycle checkpoint control, defective DNA repair pathways, and accelerated proliferation rates, normal tissue cells have intact cell cycle checkpoints and DNA repair pathways (5). In addition, some critical normal tissues are composed almost entirely of nonreplicating cells. A sensitizing agent that was effective only in cells with high replication rates and/or DNA repair defects would therefore have great clinical potential.

Poly(ADP-ribose) polymerase 1 (PARP-1) is a DNA damage sensing protein that binds to SSB (reviewed in

Authors' Affiliations: [1]Genome Damage and Stability Centre and [2]Brighton and Sussex Medical School, University of Sussex, Falmer, United Kingdom

Note: Supplementary material for this article is available at Molecular Cancer Therapeutics Online (http://mct.aacrjournals.org/).

D.A. Löser and A.K. Shibata contributed equally to this work.

Corresponding Author: Anthony J. Chalmers, Brighton and Sussex Medical School, University of Sussex, Falmer, Brighton, BN1 9RQ United Kingdom. Phone: 44-1273-876637; Fax: 44-1273-678121. E-mail: A.J.Chalmers@sussex.ac.uk

doi: 10.1158/1535-7163.MCT-09-1027

ref. 6), a process that activates its catalytic function and facilitates DNA repair. Inhibition of PARP activity reduces the rate of SSB repair and increases cellular sensitivity to ionizing radiation and alkylating agents such as methylmethane sulfonate (MMS; refs. 7–10). We have previously shown that the radiosensitizing effect of PARP inhibition requires DNA replication and that enhanced conversion of unrepaired SSB to DSB during S phase is the likely mechanism (11). Another study showed that PARP inhibition exacerbates the cytotoxicity of the alkylating agent temozolomide by enhancing conversion of SSB to DSB during S phase (12).

The cellular consequences of PARP inhibition are dictated by DNA repair proficiency. This is illustrated by the extreme sensitivity to PARP inhibitors of tumor cells deficient in BRCA1 or BRCA2 (13, 14). This phenomenon is caused by accumulation of endogenously arising DNA damage that would normally be repaired by PARP–dependent processes. In replicating cells, this damage triggers replication fork collapse, repair of which requires homologous recombination and is therefore dependent on BRCA1 and BRCA2. The impact of DNA repair defects on the sensitizing effects of PARP inhibitors in combination with DNA damaging agents remains unclear, however. Various studies have indicated that PARP inhibition exacerbates radiosensitivity (15) or chromosomal instability associated with NHEJ deficiency (16), but the evidence is inconsistent (17). Although it has been reported that PARP-1 binds to DSB and interacts with NHEJ proteins (18), there is no evidence that PARP activity is required for resolution of DSB in NHEJ proficient cells. However, an alternative repair pathway has been postulated to execute end joining of DSB in cells that are deficient in NHEJ (19). This process has been termed "backup" or "alternative" end joining, and there is evidence that it is compromised by inhibition of PARP (20). The aim of this study was to investigate the relationship between NHEJ integrity and the sensitizing effects of PARP inhibition.

NHEJ comprises core components (Ku70/80, DNA-protein kinase catalytic subunits, DNA Ligase IV, XRCC4, and XLF) that are responsible and sufficient for repair most radiation-induced DSB (reviewed in ref. 21). Loss of function of these proteins is associated with marked radiosensitivity and immunodeficiency, the latter as a consequence of impaired variable (diversity) joining recombination. A subset of radiation-induced DSB (~15%) requires more extensive processing. Repair of these breaks occurs with slow kinetics and requires additional factors, including Artemis and ataxia telangiectasia mutated (ATM). Despite the relatively small size of this subset, defects in Artemis function are associated with significant radiosensitivity (22, 23).

To elucidate the relative impact of defects in core NHEJ and the Artemis/ATM pathway on the sensitizing properties of PARP inhibition, we evaluated the effects of olaparib (AZD2281, previously KU-005946) on radiation and MMS responses in repair-defective cell lines. Olaparib is a potent and specific inhibitor of PARP-1 and PARP-2 and is currently undergoing phase II clinical trials as a single agent (24). Our data indicate that the sensitizing effects of olaparib are enhanced in cells with defective DSB repair and support the hypothesis that the sensitizing effects of PARP inhibitors will be more pronounced in tumors than in normal tissues.

Materials and Methods

Cell culture

CJ176 primary and human telomerase reverse transcriptase (hTERT; immortalized derivative) are Artemis-deficient human fibroblast cell lines. AT5-BIVA are ATM-deficient, SV40 immortalized human fibroblasts. HSC62 (kindly provided by Dr. M. Digweed) are primary fibroblasts from a patient with a homozygous mutation (IVS19-1 G to A) in BRCA2. 48BR primary and 1BR hTERT cells are wild-type (WT) controls. WT, *Artemis*$^{-/-}$, *ATM*$^{-/-}$, and *LigaseIV*$^{-/-}$*p53*$^{-/-}$ mouse embryo fibroblasts (MEF) were kind gifts from Dr. F. Alt (*Artemis*$^{-/-}$), Dr. T. Mak (WT, *ATM*$^{-/-}$), and Dr. P. McKinnon (*LigaseIV*$^{-/-}$*p53*$^{-/-}$). Human hTERT cell lines and MEFs were cultured in minimal essential medium (MEM) or α-MEM respectively, supplemented with 10% fetal calf serum, 2 mmol/L L-glutamate, penicillin (100 units/mL), and streptomycin (0.1 mg/mL). Primary cell lines and HeLa cells (obtained from ECACC) were cultured in MEM with 15% fetal calf serum. All cell culture reagents were from Gibco; other reagents were from Sigma unless otherwise stated.

Radiation and drug treatments

Cells were irradiated in medium using either a ^{137}Cs γ source (Gammacell 1000; dose rate, 7.5 Gy/min) or 250 kVp X-rays delivered at 12 mA (dose rate, 0.5 Gy/min). Olaparib (gift of KuDOS Pharmaceuticals/AstraZeneca) was used at an end concentration of 500 nmol/L, a noncytotoxic dose that abolished PARP activity in the cell lines indicated (Fig. 1A). PJ34 (Calbiochem) and KU55933 (ATM inhibitor; gift of KuDOS Pharmaceuticals/AstraZeneca) were used at end concentrations of 10 μmol/L. To inhibit DNA replication during PARP inhibition, aphidicolin (5 μmol/L) was administered for three hours, commencing 1 hour preradiation. For clonogenic survival assays using MMS, aphidicolin and olaparib were administered 1 hour before, 1 hour during, and 1 or 22 hours after treatment.

Clonogenic cell survival assay

Cells were trypsinized, seeded into 4-cm plates, and allowed to adhere at 37°C before drug treatment or irradiation. For radiation or MMS assays, cells were exposed to olaparib for 24 hours, commencing 2 hours pretreatment. For continuous olaparib exposure, medium was replaced every 48 hours to ensure constant levels of the drug. Plates were incubated at 37°C for 7 to 8 days then stained with methylene blue. Colonies of 50 cells or more were counted manually, and survival curves were derived

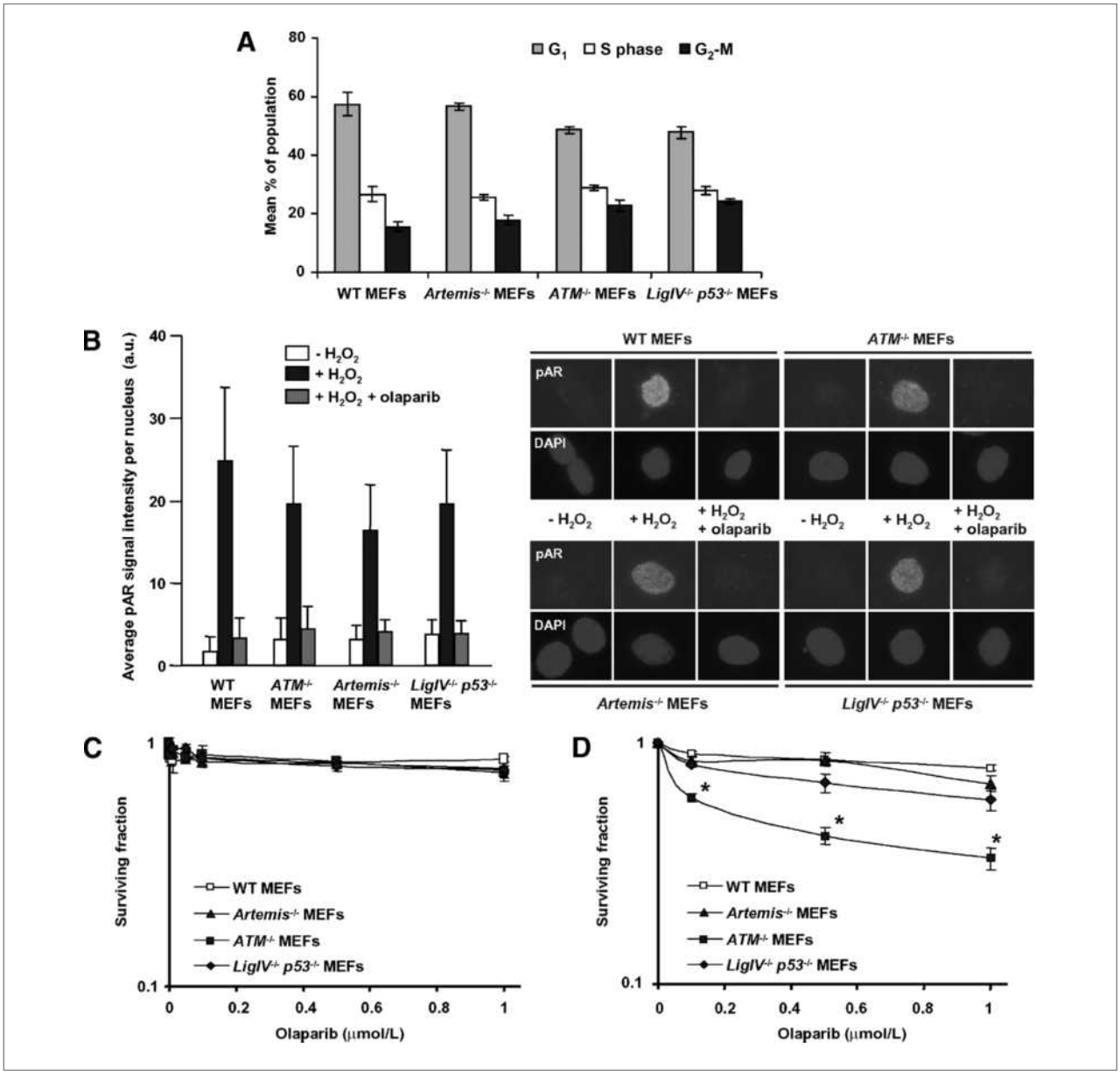

Figure 1. A, mean percentage of cells in G_1, S phase, and G_2 phases of the cell cycle in exponential phase populations of MEFs. Cells fixed and stained with propidium iodide for flow cytometric analysis of DNA content. *LigIV*$^{-/-}$, *Ligase IV*$^{-/-}$. B, WT, *ATM*$^{-/-}$, *Artemis*$^{-/-}$, and *Ligase IV*$^{-/-}$*p53*$^{-/-}$ MEFs were pretreated with 0.5 μmol/L olaparib for 2 hours before treatment with 10 mmol/L H_2O_2 (with or without 0.5 μmol/L olaparib) for 10 minutes in the dark. Cells were stained for poly(ADP-ribose) and counterstained with 4',6-diamidino-2-phenylindole. Fluorescence intensity of poly(ADP-ribose) signal in each nucleus was quantified using NIH Image-J. Mean values of 100 to 200 cells ± SD are presented. pAR, poly(ADP-ribose). C, clonogenic survival of exponential phase populations of WT, *ATM*$^{-/-}$, *Artemis*$^{-/-}$, and *Ligase IV*$^{-/-}$*p53*$^{-/-}$ MEFs exposed to olaparib at the indicated doses for 24 hours after plating. D, clonogenic survival of WT, *ATM*$^{-/-}$, *Artemis*$^{-/-}$, and *Ligase IV*$^{-/-}$*p53*$^{-/-}$ MEFs continuously exposed to olaparib for the duration of the assay. To maintain levels of olaparib, medium was replaced every 48 hours. *, $P < 0.01$ (*ATM*$^{-/-}$ compared with WT, *Artemis*$^{-/-}$, and *Ligase IV*$^{-/-}$*p53*$^{-/-}$ at each olaparib dose).

from a minimum of three independent experiments, each done in triplicate. Surviving fraction was corrected for independent cytotoxic effects of olaparib or aphidicolin, except in Supplementary Fig. S2A, wherein significant toxicity was observed. Linear quadratic (for radiation) or exponential (for MMS) models were fitted to the data sets to generate survival curves. Radiation or MMS doses associated with surviving fractions of 10%, 37%, or 50% were calculated from the fitted curves. Sensitizer enhancement ratios (SER; ref. 25) for olaparib were calculated as in Eq. 1:

$$\mathrm{SER}x = \frac{\mathrm{D}x\ (\text{no drug})}{\mathrm{D}x\ (\text{olaparib})} \qquad (1)$$

wherein Dx is the dose of ionizing radiation or MMS associated with a surviving fraction of x%. Surviving fraction after 2 Gy (SF_2) values were obtained from fitted survival data, and SF_2 ratios with and without olaparib were calculated.

Alkaline single-cell agarose gel electrophoresis (comet) assays

Alkaline comet assays were done as previously described (26). Cells suspended in medium (2.8×10^5 cells/mL) were exposed to 30-Gy γ-irradiation or to 200 μmol/L H_2O_2 for 20 minutes on ice and incubated for the indicated repair periods at 37°C in medium. Where indicated, cells were incubated with 500 nmol/L olaparib for 2 hours before DNA damage and during repair incubations. DNA strand breakage was expressed as "comet tail moment" (27). Tail moment was measured for 100 cells per sample using Comet Assay IV software (Perceptive Instruments). Average damage remaining of at least three independent experiments was calculated.

γ-H2AX foci assays

γ-H2AX foci assays were done specifically in G_1 cells as previously described (11). Cells were stained with centromere protein F (1:100; Santa Cruz) for human cells or phospho-histone H3 (1:300; Upstate Biotechnology) for mouse cells to identify G_2 phase cells. Mitotic cells were identified by morphology, and S-phase cells were identified by diffuse low-level γ-H2AX staining. Human fibroblasts (Fig. 5A) were treated with 3 μmol/L aphidicolin after irradiation to inhibit DNA replication and improve identification of S-phase cells by intensifying γ-H2AX staining (28). Thus, DSB repair in G_1 cells was monitored by enumerating γ-H2AX foci in cells that were deemed not to be in G_2, S, or mitosis.

Quantification of γ-H2AX signal and poly(ADP-ribose) signal

Slides stained as above were visualized using a Nikon Eclipse 50i microscope or a Zeiss Axioplan microscope at ×40 magnification, and image processing was done using Simple PCI software. Signal intensity within selected regions of interest was analyzed using NIH Image-J. MMS-induced γ-H2AX staining intensity was calculated by subtracting mean signal in untreated nuclei from that in MMS-treated nuclei. H_2O_2-induced poly(ADP-ribose) synthesis was measured as mean fluorescence intensity of poly(ADP-ribose) signal per nucleus.

Flow cytometric analysis of cell cycle profiles

Cells were harvested by scraping and fixed in ice-cold 70% ethanol before staining with propidium iodide (0.45 μg/mL), RNase (0.45 mg/mL), and 0.045% Tween. Resuspended cells were analyzed for DNA content on a FACS Canto flow cytometer; data was processed with FACS Diva software (Becton Dickinson).

Statistical analysis

All data were derived from at least three independent experiments. For repair foci, at least 30 nuclei were counted for each experiment, except where stated, and statistical significance was determined using Student's two-tailed t test. For clonogenic survival experiments, mean surviving fraction ± SE was plotted. SER and SF_2 values were derived from individual experiments to enable the calculation of mean values and SEM. Mean SER values were assessed for significance by Mann-Whitney U test.

Results

Sensitization to DNA damaging agents by PARP inhibition is enhanced in cells deficient in Artemis, ATM, or Ligase IV

Continuous exposure to PARP inhibition is toxic to homologous recombination–deficient cells, and shorter exposures increase the sensitivity of repair proficient cells to MMS or ionizing radiation. To investigate the influence of NHEJ on these outcomes, we tested the effect of the PARP inhibitor olaparib on survival responses of WT, Artemis, ATM, and Ligase IV–deficient MEFs. We first showed that all four cell lines were deficient in p53 protein (data not shown) and that asynchronous undamaged populations showed no significant differences in cell cycle distribution (Fig. 1A). Quantitative immunofluorescent detection of poly(ADP-ribose) synthesis after treatment with hydrogen peroxide was done (Supplementary Fig. S1), showing no significant difference in PARP activity between cells lines, and that 0.5 μmol/L olaparib inhibited PARP activity to baseline levels (Fig. 1B). Twenty-four-hour exposure to a range of olaparib doses had minimal effect on clonogenic survival (Fig. 1C), but $ATM^{-/-}$ cells were significantly more sensitive to prolonged PARP inhibition than the other cell lines (Fig. 1D; $P < 0.01$; all doses). This is consistent with previous findings (29, 30) and can be explained by the involvement of ATM in the homologous recombination pathway (29) and by defects in S-phase checkpoint signaling that have been clearly defined in ATM-deficient cells. In contrast, *Artemis*$^{-/-}$ and *Ligase IV*$^{-/-}$ cells were no more sensitive to continuous PARP inhibition than WT MEFs. Hence, NHEJ does not play an important role in repair of endogenously arising damage in replicating cells, even in the presence of PARP inhibition.

Our previous data supported the hypothesis that PARP inhibition promotes replication-dependent conversion of unrepaired SSB to potentially toxic DSB (11) To investigate whether NHEJ influences the response to these DSB, we first measured the effect of PARP inhibition and NHEJ status on sensitivity to the alkylating agent MMS, which induces predominantly SSB (Fig. 2A). WT MEFs were sensitized by PARP inhibition as expected ($SER_{37} = 2.36$), but the magnitude of this effect was markedly increased in *Artemis*$^{-/-}$ ($SER_{37} = 7.90$; $P < 0.05$) and $ATM^{-/-}$ ($SER_{37} = 4.48$; $P < 0.05$) cells (Fig. 2A; Table 1).

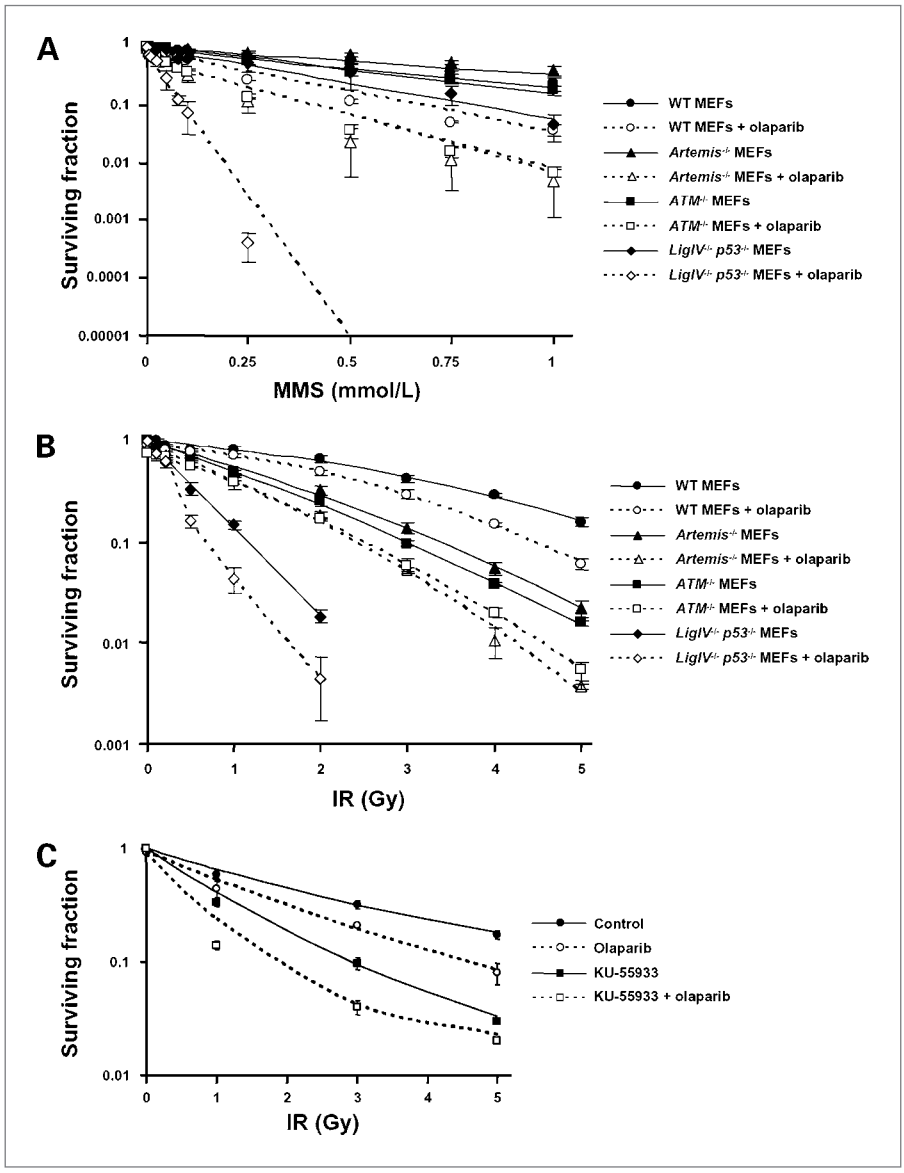

Figure 2. Clonogenic survival of exponential phase populations of WT, *ATM*$^{-/-}$, *Artemis*$^{-/-}$, and *Ligase IV*$^{-/-}$*p53*$^{-/-}$ MEFs treated with MMS for 1 hour at 37°C ± 0.5 μmol/L olaparib for 2 hours before, during, and 21 hours posttreatment (A), and 250 kV X-rays ± 0.5 μmol/L olaparib for 2 hours preirradiation and 22 hours postirradiation (B). IR, ionizing radiation. C, clonogenic survival curves derived from exponential HeLa cells exposed to 0.5 μmol/L olaparib and/or 10 μmol/L ATM inhibitor KU55933 for 2 hours preirradiation and 22 hours postirradiation.

These findings are consistent with a model whereby PARP inhibition promotes the generation of DSB from MMS-induced SSB and that these lesions are more toxic in the absence of ATM or Artemis. *Ligase IV*$^{-/-}$ cells were markedly sensitized by olaparib (SER_{37} = 14.29; P < 0.05), indicating that core NHEJ is required for repair of lesions arising under these conditions. In the absence of PARP inhibition, Ligase IV–deficient MEFs showed mild sensitivity to high doses of MMS, indicating that MMS-induced lesions, when present at high density, can generate DSB that are repaired by core NHEJ. Artemis- and ATM-deficient cells were no more sensitive to MMS than controls, indicating that MMS-induced lesions do not require processing by these proteins. The mechanisms underlying these findings are explored in more detail later.

Ionizing radiation induces DNA damage comprising SSB and DSB in a ratio of ~25:1, so the cytotoxic effects of DSB arising from SSB are obscured by those of directly induced DSB. In addition, radiation induces far fewer SSB than MMS at the doses used in these experiments. Taking this into account, the clonogenic survival data presented in Fig. 2B are consistent with the MMS observations. In the absence of olaparib, *Ligase IV*$^{-/-}$ cells were highly sensitive to radiation whereas *Artemis*$^{-/-}$ and *ATM*$^{-/-}$ cells showed intermediate sensitivity as expected. Whereas PARP inhibition had a modest radiosensitizing effect on WT MEFs (SER_{50} = 1.33), consistent with previous reports (31), higher levels of radiosensitization were observed in Artemis (SER_{50} = 1.61; P < 0.05) and Ligase IV–deficient cells (SER_{50} = 1.63; P < 0.05; Fig. 2B; Table 1). Sensitization of ATM-deficient cells was also greater than

Table 1. Mean sensitizer enhancement ratios (SER) for olaparib and mean surviving fraction at 2 Gy (SF_2) values (and SEM) calculated from clonogenic survival curves fitted with the linear quadratic model (X-rays) or the exponential model (MMS)

Cell line	Treatment					
	X-ray					MMS
	SER_{37}	SER_{50}	Mean SF_2	Mean SF_2 olaparib	Ratio	SER_{37}
WT MEFs	1.30 (0.01)	1.33 (0.01)	0.62 (0.04)	0.49 (0.07)	1.27	2.36 (0.28)
ATM$^{-/-}$ MEFs	1.34 (0.11)	1.56 (0.15)	0.23 (0.007)	0.17 (0.02)	1.35	4.48* (0.14)
Artemis$^{-/-}$ MEFs	1.50* (0.06)	1.61* (0.08)	0.29 (0.02)	0.16 (0.02)	1.81	7.90* (0.91)
LigIV$^{-/-}$ *p53*$^{-/-}$ MEFs	1.66* (0.02)	1.63* (0.06)	0.02 (-)	0.004 (-)	4.22	14.29* (2.99)
HeLa control	1.50 (0.11)	1.50 (0.11)	0.45 (0.04)	0.32 (0.03)	1.41	—
HeLa +KU-5933	1.75 (0.08)	1.87 (0.07)	0.19 (0.02)	0.09 (0.01)	2.15	—

NOTE: *P* values calculated for comparisons between WT and DNA repair–defective cell lines.
*$P < 0.05$.

in WT cells, but this did not reach statistical significance (SER_{50} = 1.56).

To validate the relevance of these findings to the treatment of cancer, the impact of the ATM inhibitor KU-55933 on the radiosensitizing effects of olaparib was measured in HeLa cells. The magnitude of the sensitizing effect of olaparib was enhanced on a background of ATM inhibition (SER_{50} = 1.87 compared with 1.50; Fig. 2C; Table 1). For additional clinical relevance, surviving fractions at 2 Gy (SF_2) were calculated for all survival

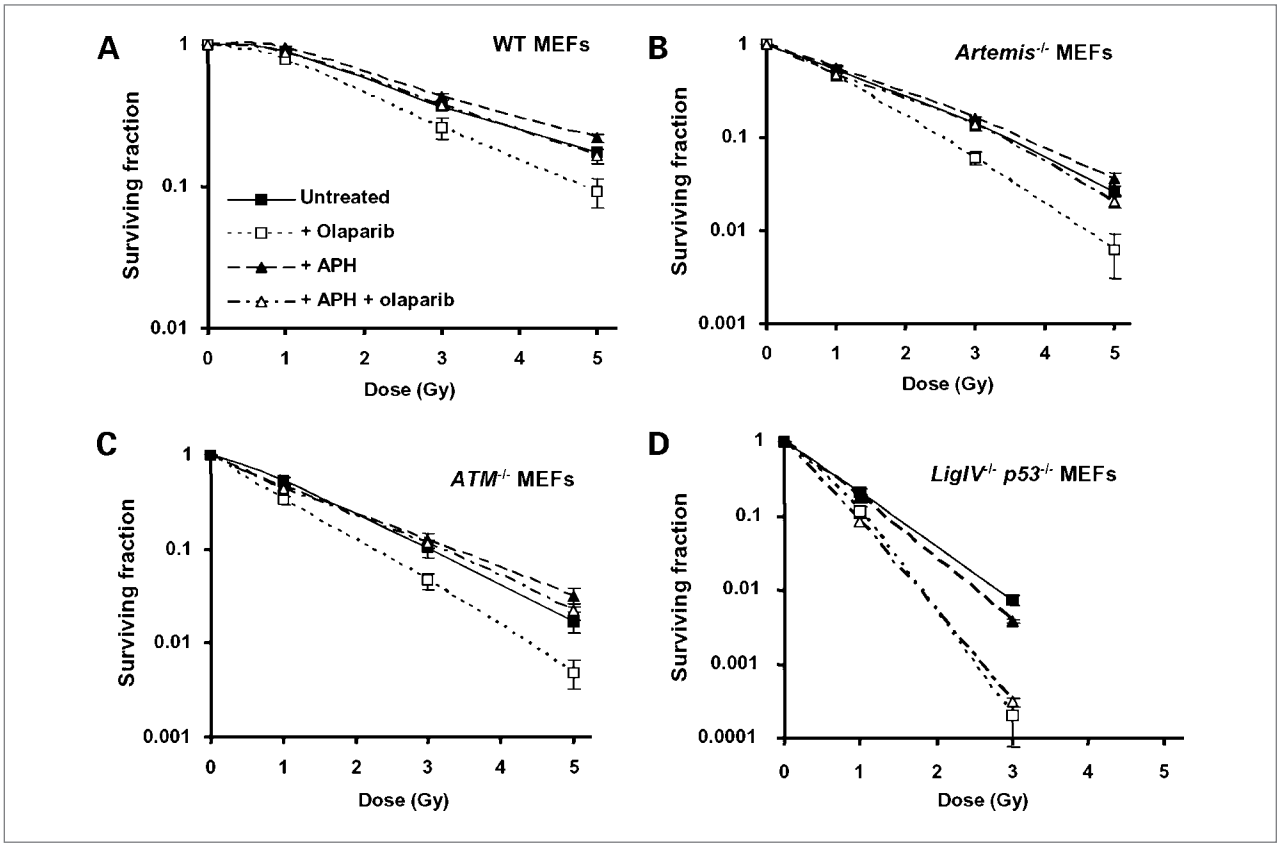

Figure 3. Clonogenic survival curves derived from MEFs exposed to 0.5 μmol/L olaparib and/or 5 μmol/L aphidicolin for 1 hour preirradiation and 2 hours postirradiation with 250 kV X-rays at the doses shown. A, WT MEFs. B, *Artemis*$^{-/-}$ MEFs. C, *ATM*$^{-/-}$ MEFs. D, *Ligase IV*$^{-/-}$*p53*$^{-/-}$ MEFs.

experiments and SF_2 ratios in the presence and absence of olaparib derived (Table 1). In all cases, the ratio was markedly increased in DNA repair–defective backgrounds, with the greatest effect observed in Ligase IV–deficient MEFs.

Radiosensitization associated with PARP inhibition is replication dependent in Artemis and ATM but not Ligase IV–deficient cells

To investigate whether the radiosensitizing effects of olaparib in NHEJ-deficient cells are mediated by replication-dependent conversion of SSB to DSB, the DNA polymerase inhibitor aphidicolin was used to inhibit DNA replication during the period of PARP inhibition. Radiosensitization by olaparib was completely rescued by aphidicolin in WT, *Artemis*$^{-/-}$, and *ATM*$^{-/-}$ cells (Fig. 3A-C) but was unaffected in Ligase IV–deficient cells (Fig. 3D). This indicates that DNA replication is not necessary for radiosensitization of Ligase IV–defective cells.

To eliminate the possibility that the sensitizing effects of PARP inhibition in ATM- and Artemis-deficient cells might reflect direct involvement of either protein in SSB repair, alkaline comet assays were done in *ATM*$^{-/-}$ and *Artemis*$^{-/-}$ MEFs (Supplementary Fig. S2). Both cell lines exhibited normal repair kinetics after treatment with ionizing radiation or the SSB-inducing agent hydrogen peroxide. Addition of olaparib delayed repair as expected, but the effect was no greater in ATM- or Artemis-deficient cells than in WT controls. Together with the replication-dependent effect on survival, these observations implicate increased conversion of SSB to cytotoxic DSB during DNA replication as the primary mechanism underlying the enhanced radiosensitizing effect of PARP inhibition in *ATM*$^{-/-}$ and *Artemis*$^{-/-}$ cells.

Resolution of DNA damage induced by MMS and PARP inhibition during S phase is delayed in Artemis-deficient cells.

We hypothesized that the increased effects of PARP inhibition in Artemis-deficient cells were a consequence of defective repair of replication-dependent DSB. To verify this, we exposed cells to MMS and quantified levels of phosphorylated histone H2AX (γ-H2AX) immunofluorescence in S-phase MEFs. In G_0 and G_1 cells γ-H2AX foci have been shown to correlate well with DSB numbers as measured by neutral comet assay, pulsed field gel electrophoresis, and survival after ionizing radiation (32). However, phosphorylation of H2AX also occurs diffusely in response to damage other than DSB and during apoptosis and may be stimulated by replication fork collapse. As a result, individual γ-H2AX foci cannot be accurately detected in S-phase cells. To quantify replication-associated DNA damage, therefore, we analyzed total γ-H2AX staining intensity in S-phase nuclei. These were identified by negative phospho-histone H3 and diffuse γ-H2AX staining (28). In combination with MMS, PARP inhibition increased total γ-H2AX signal in WT and *Artemis*$^{-/-}$ cells, with similar increases occurring up to 4 hours after MMS treatment. At 24 hours, however, S-phase *Artemis*$^{-/-}$ cells exhibited significantly greater γ-H2AX signal than WT (Fig. 4A; quantified in Fig. 4B; $P < 0.05$), indicating impaired resolution of damage. By measuring γ-H2AX staining intensity in phospho-histone H3–positive cells, we showed that the excess damage persisted as cells progressed into G_2 (Fig. 4C), with *Artemis*$^{-/-}$ cells staining much more intensely than WT ($P < 0.05$ at 24 hours; Fig. 4C and D). These findings are consistent with the clonogenic survival data (Fig. 2A) and support the hypothesis that PARP inhibition promotes replication-associated conversion of SSB to DSB that require Artemis for efficient repair.

PARP inhibition increases radiation sensitivity in NHEJ-deficient cells by obstructing an alternative end-joining pathway

Survival data indicated that DNA replication was not required for radiosensitization of Ligase IV–deficient cells by olaparib (Fig. 3D). To explore replication-independent mechanisms, we measured the effect of PARP inhibition on induction and resolution of γ-H2AX foci after ionizing radiation, specifically in G1 phase nuclei. Cells were costained for centromere protein F (human fibroblasts) or phospho-histone H3 (MEFs) to identify G_2 (centromere protein F or phospho-histone H3 positive) and G_1 (centromere protein F or phospho-histone H3 negative) nuclei (28). S-phase nuclei were identified by intermediate centromere protein F staining (human cells) and diffuse background γH2AX staining. Mitotic or apoptotic cells were identified by their distinctive 4′,6-diamidino-2-phenylindole staining pattern. By excluding these nuclei, the specificity of the γH2AX foci assay for true DSB was increased. To further substantiate DSB specificity, we showed that the induction of γ-H2AX foci by ionizing radiation was abolished by simultaneous inhibition of the DSB-dependent kinases ATM and DNA-PK in human fibroblasts and MEFs (Supplementary Fig. S3A and B). Hence, although ionizing radiation induces high levels of both SSB and DSB, H2AX phosphorylation occurs only in response to signaling events that are specifically activated by DSB.

As reported previously (33), G_1 phase Artemis- and ATM-deficient cells exhibited a partial DSB repair defect (Fig. 5A). PARP inhibition did not affect induction or resolution of γ-H2AX foci, consistent with the model that DNA replication is required to generate excess double-stranded lesions in these cell lines.

G_1 phase Ligase IV– and Ku80-deficient cells exhibited a more marked but not complete DSB repair defect (Fig. 5B). In these cells, PARP inhibition significantly increased the number of persistent γ-H2AX foci (Fig. 5B; $P < 0.01$ at 4 and 8 h for *Ligase IV*$^{-/-}$ cells; $P < 0.05$ and $P < 0.01$ at 4 and 8 h, respectively, for *Ku80*$^{-/-}$ cells). Indeed, residual DSB repair function seemed to be abolished by PARP inhibition in these NHEJ-deficient

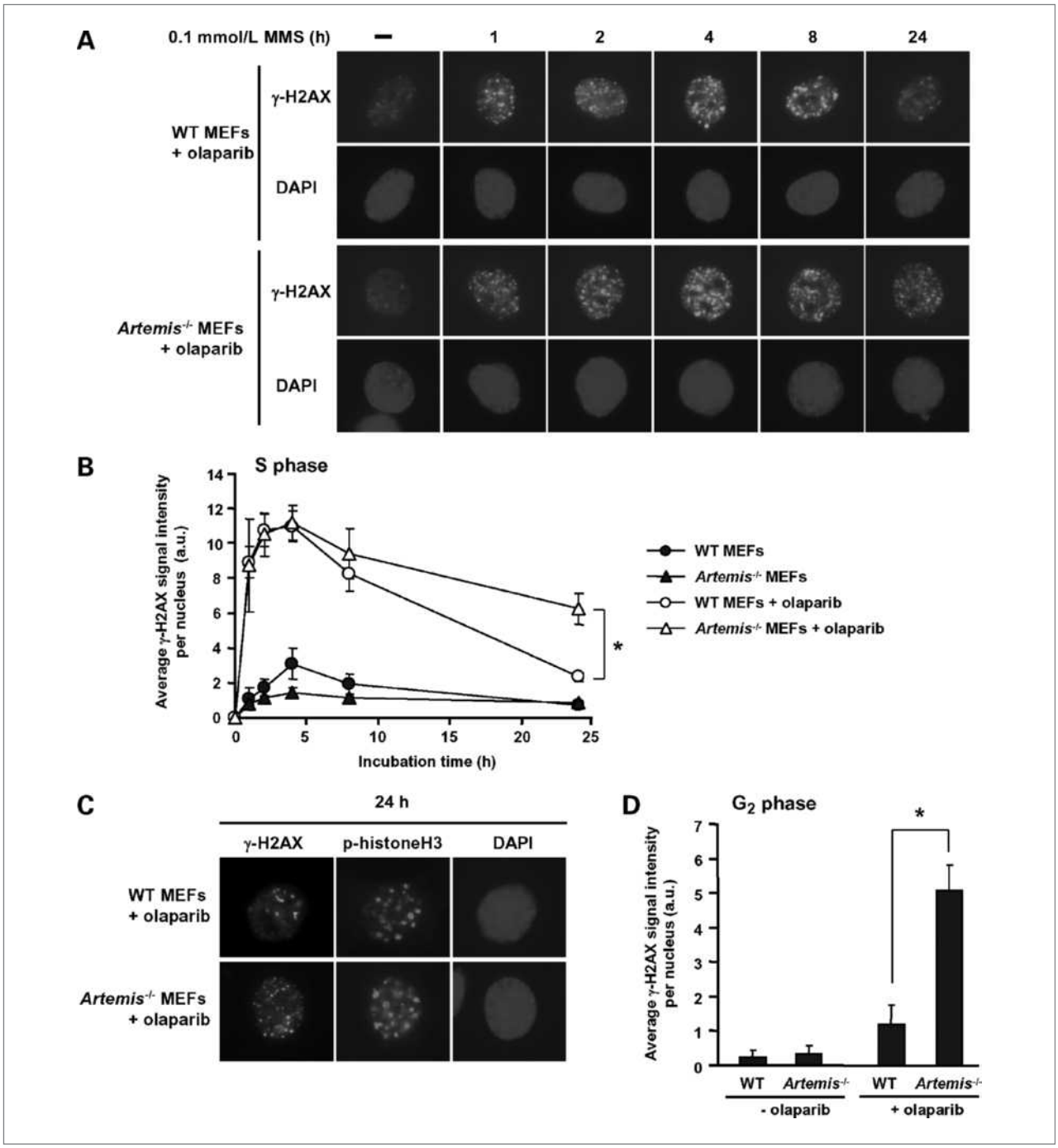

Figure 4. A, representative images of γH2AX immunofluorescence in S-phase WT or *Artemis*$^{-/-}$ MEFs. Cells were exposed to 0.5 μmol/L olaparib for 1 hour before treatment with MMS (0.1 mmol/L, 1 h) and until fixation at the time points shown. DAPI, 4',6-diamidino-2-phenylindole. B, quantitative analysis of γH2AX signal in S-phase WT or *Artemis*$^{-/-}$ MEFs. Mean fluorescence intensity per nucleus ± SE from three experiments; at least 25 nuclei per time point. *, $P < 0.05$. C, representative images of γH2AX and phospho-histone H3 immunofluorescence in G_2-phase WT and *Artemis*$^{-/-}$ MEFs 24 hours after MMS ± olaparib treatment as in A. G_2-phase cells were identified by speckled p-histone H3 staining. p-histoneH3, phospho-histone H3. D, quantitative analysis of γH2AX signal in G_2-phase cells 24 hours after MMS treatment ± olaparib. *, $P < 0.05$.

cells. This supports the hypothesis that the activity of an alternative end-joining pathway is promoted in the absence of either Ku80 or Ligase IV and eliminated by inhibition of PARP (20, 34).

To exclude the possibility that these observations reflected effects on H2AX phosphorylation or focus dynamics rather than DSB repair, we showed that treatment with the PARP inhibitor did not affect the number of foci

induced by irradiation (Supplementary Fig. S4A), the rate at which they resolved (Fig. 5A and Supplementary Fig. S4A), or the signal intensity per focus at 30 minutes or 8 hours after irradiation (Supplementary Fig. S4B and C).

PARP inhibition promotes replication independent accumulation of DSB in MMS-treated Ligase IV–deficient cells

Our observation that *Ligase IV*$^{-/-}$ cells were sensitive to high doses of MMS in the absence of PARP inhibition (Fig. 2A) and were more profoundly sensitized to MMS by PARP inhibition than other repair-defective cells raised the possibility that additional mechanisms might be operating. We hypothesized that PARP inhibition would delay repair of SSB induced by MMS and increase the probability of unrepaired lesions giving rise to DSB by interacting either with adjacent SSB or with transcription machinery (35). Either mechanism might be exacerbated by persistent binding of inhibited PARP at the damaged sites. To investigate this hypothesis, we monitored the appearance of γ-H2AX foci in WT and repair-deficient cells. Effects of DNA replication were eliminated by restricting the analysis to cells in G_1 phase, and the specificity of γ-H2AX foci for DSB was validated as described above and illustrated in Supplementary Fig. S3.

PARP inhibition was required for generation of γ-H2AX foci in G_1 phase WT fibroblasts exposed to MMS for 1 hour (Fig. 6A; Supplementary Fig. S5). PARP inhibition significantly increased DSB formation between 1 and 4 hours after MMS treatment ($P < 0.001$, $P < 0.05$, and $P < 0.01$ at 1, 2, and 4 h, respectively; Fig. 6B). In WT cells, γ-H2AX foci were few (6-8 per cell) and were almost completely repaired within 8 hours (Fig. 6B), but in Ligase IV–deficient MEFs, foci continued to accumulate over 8 hours (Fig. 6C). This accumulation was observed in the presence and absence of the PARP inhibitor, but the increase in foci associated with PARP inhibition was much greater than in WT cells and was highly significant ($P < 0.05$ at 1 h; $P < 0.001$ at 2, 4, and 8 h). At 24 hours, cells exhibited intense γ-H2AX staining indicative of apoptosis and foci could not be counted. In G_1-phase Artemis-deficient human fibroblasts (CJ176), the kinetics of induction and repair of γ-H2AX foci were essentially normal and the effect of PARP inhibition was no greater than in WT fibroblasts (Fig. 6D), indicating that DNA replication is required to generate DSB that are substrates for Artemis. Similarly, BRCA2-mutant homologous recombination–defective cells (HSC62) showed

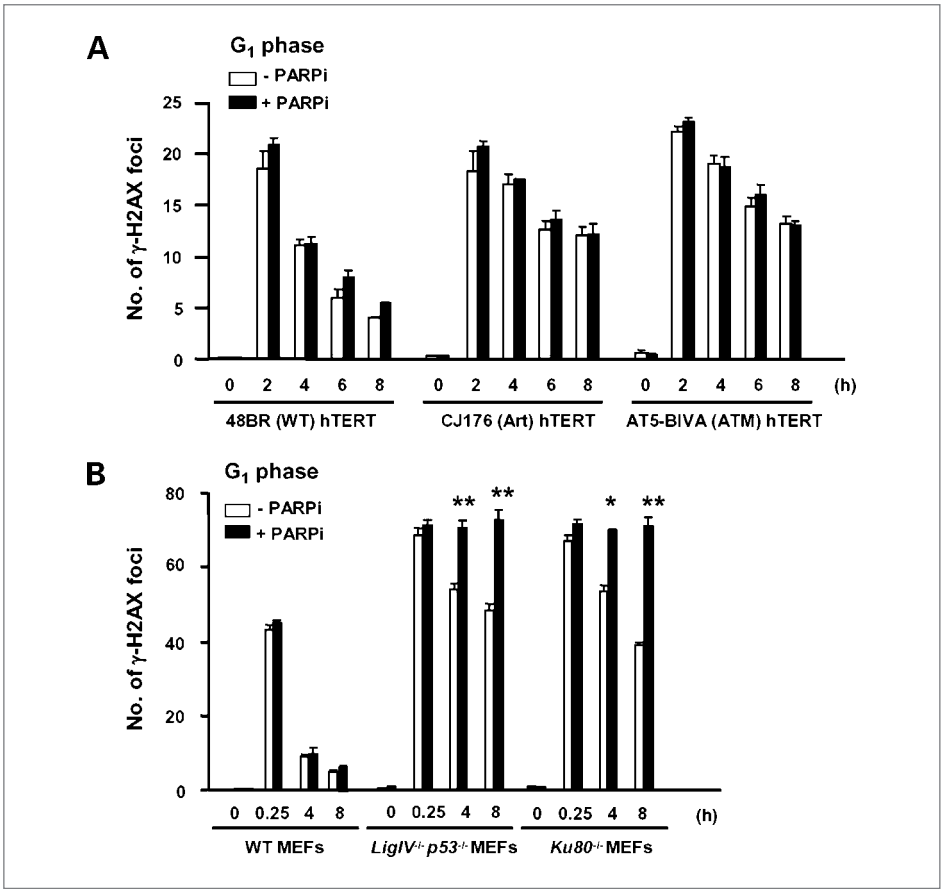

Figure 5. A, quantitative analysis of γH2AX foci in G_1 phase 48BR hTERT (WT), CJ176 hTERT (Artemis deficient), and AT5-BIVA hTERT (ATM deficient) fibroblast cell lines exposed to 10 μmol/L PJ-34 (PARP inhibitor) for 1 hour preirradiation (3 Gy; γ rays), treated with 3 μmol/L aphidicolin, and then fixed and costained for γH2AX and centromere protein F. PARPi, PARP inhibitor. B, quantitative analysis of γ-H2AX foci in G_1 phase MEFs exposed to 10 μmol/L PJ-34 for 1 hour preirradiation (3 Gy; γ rays), fixed, and stained for γ-H2AX and phospho-histone H3. G_2 cells distinguished by phospho-histone H3 staining and S-phase cells identified by background γ-H2AX staining were excluded. *, $P < 0.05$; **, $P < 0.01$ for comparison between cells treated or not with PARP inhibitor.

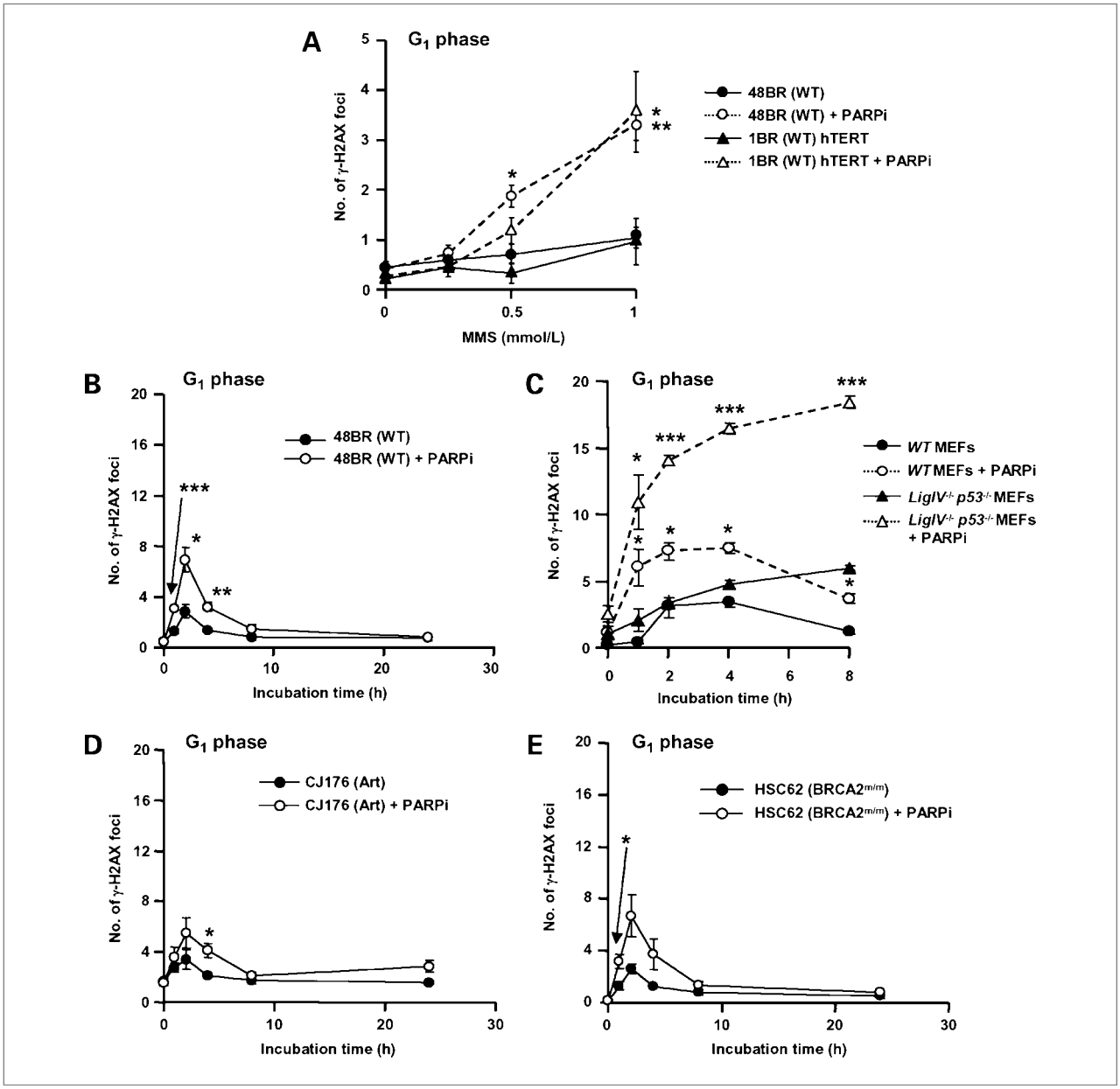

Figure 6. A, quantitative analysis of γH2AX foci in G_1 phase 48BR primary and 1BR hTERT fibroblasts exposed to 10 μmol/L PJ-34 for 1 hour before treatment with MMS at the indicated doses. B-E, quantitative analysis of γH2AX foci in 48BR (B), *Ligase IV*$^{-/-}$*p53*$^{-/-}$ MEFs (C), CJ176 (Artemis deficient; D), and HSC62 (BRCA2 deficient; E) primary fibroblast cell lines and exposed to 10 μmol/L PJ-34 for 1 hour before and during damage induction with 1 mmol/L MMS and for the indicated repair periods. Cells were fixed and costained for γH2AX and centromere protein F or phospho-histone H3. *, $P < 0.05$; **, $P < 0.01$; ***, $P < 0.001$ for comparison between cells treated or not with PARP inhibitor. Representative images are shown in Supplementary Fig. S5.

normal DSB repair kinetics and the same response to PARP inhibition as WT (Fig. 6E). Hence, DSB arising from MMS-induced damage in the absence of replication are repaired by Ligase IV–dependent NHEJ.

These data show that treatment with MMS yields low levels of DSB, most of which are not normally detected because they are rapidly repaired by core NHEJ. In the presence of a PARP inhibitor, DSB induction is greatly increased and these lesions are also repaired by Ligase IV–dependent NHEJ. These novel observations provide a possible explanation for the relative sensitivity of *Ligase IV*$^{-/-}$ MEFs to high doses of MMS and the gross sensitizing effect of PARP inhibition (Fig. 2A).

Discussion

PARP inhibitors have clinical potential as sensitizers to be used in combination with ionizing radiation or with

alkylating agents. It is important to establish whether these effects will be tumor specific and whether therapeutic benefit can be predicted by the integrity of DNA repair pathways in the target tumor. Our previous study showed that radiosensitization of human tumor cells is replication dependent and mediated primarily through conversion of unrepaired SSB to DSB during DNA replication (11). Here, we show that sensitization to ionizing radiation and the alkylating agent MMS is enhanced in DSB repair–defective cells. Both findings predict that the sensitizing effects of PARP inhibitors will be more pronounced in tumors than in normal tissues. Furthermore, we show that the mechanisms responsible for sensitization differ between *Ligase IV*$^{-/-}$ cells and *Artemis*$^{-/-}$ or *ATM*$^{-/-}$ cells and provide evidence for distinct mechanisms by which PARP inhibition increases unrepaired DSB after induction of single stranded DNA damage.

Replication-dependent effects of PARP inhibition: ionizing radiation and MMS

In this study, we examined the effect of PARP inhibition on MMS sensitivity and observed a markedly greater effect in *Artemis*$^{-/-}$ or *ATM*$^{-/-}$ cells than in DSB repair–proficient cells. The radiosensitizing effects of PARP inhibition were also enhanced in Artemis- and ATM-deficient cells than WT, but the differential effect was less marked, probably because ionizing radiation induces a spectrum of damage that includes SSB and DSB. Radiosensitization was replication dependent in WT, *Artemis*$^{-/-}$, or *ATM*$^{-/-}$ cells. These observations are consistent with a model in which the primary effect of PARP inhibition is to abrogate SSB repair, leading to the replication-dependent generation of cytotoxic DSB, repair of which is inhibited in the absence of Artemis or ATM.

ATM might promote repair of replication-dependent DSB by a variety of mechanisms. These include initiation of cell cycle checkpoints, activation of homologous recombination repair of replication coupled DSB (29), and promotion by phosphorylation of the end-processing activity of Artemis (33). Likewise, Artemis has established roles in end-processing of complex DSB and resolving hairpin structures during variable (diversity) joining recombination (36). Because PARP inhibition causes persistent binding of PARP to damaged DNA (37), it is also possible that the nuclease activity of Artemis is required to remove the PARP-DNA complex and allow repair. Our data indicate that such a requirement may be particularly marked in the context of DNA replication.

Replication-independent effects of PARP inhibition: ionizing radiation

It has been proposed that an alternative end-joining pathway functions in the absence of classic NHEJ (20). To consolidate the concept that this pathway is compromised by PARP inhibition, we analyzed induction and repair of γ-H2AX foci after low doses of radiation. To eliminate the effects of homologous recombination in S and G_2 phase, foci were enumerated in G_1 cells only. Consistent with previous findings, PARP inhibition blocked DSB repair in *Ku80*$^{-/-}$ and *Ligase IV*$^{-/-}$ cells. These data support the previously proposed model whereby Ku and PARP compete for binding at DSB ends (20) and provide an explanation for our observation that radiosensitization of Ligase IV–deficient cells by PARP inhibition is more pronounced than in WT cells and is independent of DNA replication.

In this study, we also show for the first time that PARP inhibition has no direct impact on DSB repair in Artemis- and ATM-defective G_1 cells, following exposure to ionizing radiation. This is consistent with our observation that sensitization to DNA damaging agents by PARP inhibition is replication dependent in *Artemis*$^{-/-}$ and *ATM*$^{-/-}$ cells and shows that the activity of the alternative end-joining pathway is not promoted by the absence of Artemis or ATM. It also supports the idea that Ku binding activity at DSB is unaffected by the absence of these repair factors. Of note, these results do not necessitate that PARP plays a functional role in alternative end joining. The data show only that inhibition of PARP can block the activity of this process.

Replication-independent effects of PARP inhibition: MMS

PARP inhibition caused gross sensitization of *Ligase IV*$^{-/-}$ cells to MMS. This was unexpected because MMS is not thought to induce significant numbers of DSB directly. To investigate whether MMS treatment generates DSB in the absence of DNA replication and the role of PARP inhibition in this process, γ-H2AX foci were enumerated in G_1 cells. Ligase IV–deficient cells exhibited significant accumulation of DSB (18 per G_1 nucleus), following exposure to 1 mmol/L MMS in the presence of a PARP inhibitor. This indicates that PARP inhibition promotes replication independent generation of DSB from MMS-induced lesions and that these DSB require core NHEJ for repair. Such DSB might arise from overlapping SSB or from interactions between transcription and obstructed SSB. Low numbers of γ-H2AX foci (7 per G_1 nucleus) were detected in WT cells exposed to MMS in combination with the PARP inhibitor, again indicating that MMS is capable of inducing replication-independent DSB when base excision repair is impaired. In NHEJ proficient cells, however, these DSB were rapidly repaired.

A previous study failed to detect induction of DSB following exposure to MMS (38). This discrepancy may be explained by the increased sensitivity of the γ-H2AX foci assay compared with pulsed-field gel electrophoresis, which has a detection limit of ~300 DSB (equivalent to at least 10 Gy in G_1 cells). The γ-H2AX foci assay is highly sensitive but must be used with caution because of the ability of DNA lesions other than DSB to stimulate phosphorylation of H2AX. Its validity in these experiments is supported by the fact that induction of foci by MMS was entirely abolished by inhibition of ATM and DNA-PK because phosphorylation of H2AX by these two proteins occurs only when they are activated by the presence of

DNA DSB (39). In addition, resolution of the γ-H2AX foci induced by MMS was Ligase IV dependent. In support of our observations, Woodhouse and colleagues (40) have shown that hydrogen peroxide treatment generates DSB in PARP-1–deficient but not control cells. Our study extends this finding by showing that SSB are converted into DSB in the absence of DNA replication and that the resulting DSB require NHEJ for repair. Artemis- and BRCA2-deficient cells exhibited normal repair of DSB under these conditions. Hence, in Ligase IV–deficient cells, inhibition of PARP acts through two distinct replication-independent mechanisms to increase the cytotoxic effects of SSB-inducing agents such as MMS and ionizing radiation.

Relevance to cancer therapy

The capacity of PARP inhibitors to increase tumor radiosensitivity has been shown in a number of *in vitro* and *in vivo* models (41, 42), and the low toxicity of these compounds predicts a beneficial clinical response. However, the major impediment to clinical use of radiosensitizing agents is parallel sensitization of normal tissues (43). In this study, we have shown that the sensitizing effects of PARP inhibitors are manifested only in replicating cells or in nonreplicating cells that are deficient in core NHEJ proteins. Sensitization to ionizing radiation, particularly to the alkylating agent MMS, was enhanced in cells deficient in the "noncore" NHEJ-repair proteins ATM and Artemis. Tumors exhibiting defective NHEJ repair may therefore be particularly sensitive to PARP inhibitors in combination with radiation or alkylating chemotherapy agents. In general, tumor cells are characterized by higher rates of replication than normal tissues and are much more likely to exhibit defective DNA repair (5, 44). Furthermore, specific defects in NHEJ have been documented in high-grade malignancies such as carcinoma of the bladder (45) and glioblastoma multiforme (46), and ATM deficiency is a feature of mantle cell lymphoma (47). Thus, it is likely that the radiosensitizing effects of PARP inhibitors such as olaparib will be more marked in tumor cells than in adjacent normal tissues. The resulting therapeutic benefit may be particularly apparent in the case of brain tumors, where the critical normal tissue, the brain, is composed predominantly of nonreplicating cells with intact DNA repair pathways (48).

Disclosure of Potential Conflicts of Interest

No potential conflicts of interest were disclosed.

Acknowledgments

We thank Graeme Smith and Niall Martin at KuDOS Pharmaceuticals (AstraZeneca) for the helpful discussion and for providing olaparib and KU-55933.

Grant Support

Medical Research Council Clinician Scientist Fellowship (G108/589; A.J. Chalmers and D.A. Löser), Medical Research Council Programme Grant (G0500897; P.A. Jeggo and A. Shibata), and JSPS Research Fellowship for Young Scientists (A. Shibata).

The costs of publication of this article were defrayed in part by the payment of page charges. This article must therefore be hereby marked *advertisement* in accordance with 18 U.S.C. Section 1734 solely to indicate this fact.

Received 11/04/2009; revised 03/25/2010; accepted 04/16/2010; published OnlineFirst 06/08/2010.

References

1. Goodhead DT. Initial events in the cellular effects of ionizing radiations: clustered damage in DNA. Int J Radiat Biol 1994;65:7–17.
2. Rothkamm K, Kruger I, Thompson LH, Lobrich M. Pathways of DNA double-strand break repair during the mammalian cell cycle. Mol Cell Biol 2003;23:5706–15.
3. Koch CA, Agyei R, Galicia S, et al. Xrcc4 physically links DNA end processing by polynucleotide kinase to DNA ligation by DNA ligase IV. EMBO J 2004;23:3874–85.
4. Radford IR. The level of induced DNA double-strand breakage correlates with cell killing after X-irradiation. Int J Radiat Biol Relat Stud Phys Chem Med 1985;48:45–54.
5. Martin SA, Lord CJ, Ashworth A. DNA repair deficiency as a therapeutic target in cancer. Curr Opin Genet Dev 2008;18:80–6.
6. D'Amours D, Desnoyers S, D'Silva I, Poirier GG. Poly(ADP-ribosyl)ation reactions in the regulation of nuclear functions. Biochem J 1999;342:249–68.
7. Dantzer F, de La Rubia G, Menissier-De Murcia J, Hostomsky Z, de Murcia G, Schreiber V. Base excision repair is impaired in mammalian cells lacking poly(ADP-ribose) polymerase-1. Biochemistry 2000;39:7559–69.
8. Trucco C, Oliver FJ, de Murcia G, Menissier-de Murcia J. DNA repair defect in poly(ADP-ribose) polymerase-deficient cell lines. Nucleic Acids Res 1998;26:2644–9.
9. Fisher AE, Hochegger H, Takeda S, Caldecott KW. Poly(ADP-ribose) polymerase 1 accelerates single-strand break repair in concert with poly(ADP-ribose) glycohydrolase. Mol Cell Biol 2007;27:5597–605.
10. de Murcia JM, Niedergang C, Trucco C, et al. Requirement of poly(ADP-ribose) polymerase in recovery from DNA damage in mice and in cells. Proc Natl Acad Sci U S A 1997;94:7303–7.
11. Dungey FA, Loser DA, Chalmers AJ. Replication-dependent radiosensitization of human glioma cells by inhibition of poly(ADP-Ribose) polymerase: mechanisms and therapeutic potential. Int J Radiat Oncol Biol Phys 2008;72:1188–97.
12. Liu X, Shi Y, Guan R, et al. Potentiation of temozolomide cytotoxicity by poly(ADP)ribose polymerase inhibitor ABT-888 requires a conversion of single-stranded DNA damages to double-stranded DNA breaks. Mol Cancer Res 2008;6:1621–9.
13. Bryant HE, Schultz N, Thomas HD, et al. Specific killing of BRCA2-deficient tumours with inhibitors of poly(ADP-ribose) polymerase. Nature 2005;434:913–7.
14. Farmer H, McCabe N, Lord CJ, et al. Targeting the DNA repair defect in BRCA mutant cells as a therapeutic strategy. Nature 2005;434:917–21.
15. Veuger SJ, Curtin NJ, Richardson CJ, Smith GC, Durkacz BW. Radiosensitization and DNA repair inhibition by the combined use of novel inhibitors of DNA-dependent protein kinase and poly(ADP-ribose) polymerase-1. Cancer Res 2003;63:6008–15.
16. Tong WM, Cortes U, Hande MP, et al. Synergistic role of Ku80 and poly(ADP-ribose) polymerase in suppressing chromosomal aberrations and liver cancer formation. Cancer Res 2002;62:6990–6.

17. Noel G, Giocanti N, Fernet M, Megnin-Chanet F, Favaudon V. Poly (ADP-ribose) polymerase (PARP-1) is not involved in DNA double-strand break recovery. BMC Cell Biol 2003;4:7.
18. Li B, Navarro S, Kasahara N, Comai L. Identification and biochemical characterization of a Werner syndrome protein complex with Ku70/80 and PARP-1. J Biol Chem 2004;279:13659–67.
19. Corneo B, Wendland RL, Deriano L, et al. Rag mutations reveal robust alternative end joining. Nature 2007;449:483–6.
20. Wang M, Wu W, Rosidi B, Zhang L, Wang H, Iliakis G. PARP-1 and Ku compete for repair of DNA double strand breaks by distinct NHEJ pathways. Nucleic Acids Res 2006;34:6170–82.
21. Lieber MR, Lu H, Gu J, Schwarz K. Flexibility in the order of action and in the enzymology of the nuclease, polymerases, and ligase of vertebrate non-homologous DNA end joining: relevance to cancer, aging, and the immune system. Cell Res 2008;18:125–33.
22. Moshous D, Callebaut I, de Chasseval R, et al. Artemis, a novel DNA double-strand break repair/V(D)J recombination protein, is mutated in human severe combined immune deficiency. Cell 2001;105:177–86.
23. Rooney S, Alt FW, Lombard D, et al. Defective DNA repair and increased genomic instability in Artemis-deficient murine cells. J Exp Med 2003;197:553–65.
24. Fong PC, Boss DS, Yap TA, et al. Inhibition of poly(ADP-ribose) polymerase in tumors from BRCA mutation carriers. N Engl J Med 2009;361:123–34.
25. McCulloch EA, Till JE. The sensitivity of cells from normal mouse bone marrow to γ radiation *in vitro* and *in vivo*. Radiat Res 1962; 16:822–32.
26. Breslin C, Clements PM, El-Khamisy SF, Petermann E, Iles N, Caldecott KW. Measurement of chromosomal DNA single-strand breaks and replication fork progression rates. Methods Enzymol 2006;409:410–25.
27. Olive PL, Banath JP, Durand RE. Heterogeneity in radiation-induced DNA damage and repair in tumor and normal cells measured using the "comet" assay. Radiat Res 1990;122:86–94.
28. Deckbar D, Birraux J, Krempler A, et al. Chromosome breakage after G2 checkpoint release. J Cell Biol 2007;176:749–55.
29. Bryant HE, Helleday T. Inhibition of poly (ADP-ribose) polymerase activates ATM which is required for subsequent homologous recombination repair. Nucleic Acids Res 2006;34:1685–91.
30. Aguilar-Quesada R, Munoz-Gamez JA, Martin-Oliva D, et al. Interaction between ATM and PARP-1 in response to DNA damage and sensitization of ATM deficient cells through PARP inhibition. BMC Mol Biol 2007;8:29.
31. Shall S, de Murcia G. Poly(ADP-ribose) polymerase-1: what have we learned from the deficient mouse model? Mutat Res 2000;460:1–15.
32. Rothkamm K, Lobrich M. Evidence for a lack of DNA double-strand break repair in human cells exposed to very low x-ray doses. Proc Natl Acad Sci U S A 2003;100:5057–62.
33. Riballo E, Kuhne M, Rief N, et al. A pathway of double-strand break rejoining dependent upon ATM, Artemis, and proteins locating to γ-H2AX foci. Mol Cell 2004;16:715–24.
34. Hochegger H, Dejsuphong D, Fukushima T, et al. Parp-1 protects homologous recombination from interference by Ku and Ligase IV in vertebrate cells. EMBO J 2006;25:1305–14.
35. Wu J, Liu LF. Processing of topoisomerase I cleavable complexes into DNA damage by transcription. Nucleic Acids Res 1997;25: 4181–6.
36. Ma Y, Pannicke U, Schwarz K, Lieber MR. Hairpin opening and overhang processing by an Artemis/DNA-dependent protein kinase complex in nonhomologous end joining and V(D)J recombination. Cell 2002;108:781–94.
37. Godon C, Cordelieres FP, Biard D, et al. PARP inhibition versus PARP-1 silencing: different outcomes in terms of single-strand break repair and radiation susceptibility. Nucleic Acids Res 2008; 36:4454–64.
38. Lundin C, North M, Erixon K, et al. Methyl methanesulfonate (MMS) produces heat-labile DNA damage but no detectable *in vivo* DNA double-strand breaks. Nucleic Acids Res 2005;33:3799–811.
39. Stiff T, O'Driscoll M, Rief N, Iwabuchi K, Lobrich M, Jeggo PA. ATM and DNA-PK function redundantly to phosphorylate H2AX after exposure to ionizing radiation. Cancer Res 2004;64:2390–6.
40. Woodhouse BC, Dianova II, Parsons JL, Dianov GL. Poly(ADP-ribose) polymerase-1 modulates DNA repair capacity and prevents formation of DNA double strand breaks. DNA Repair (Amst) 2008; 7:932–40.
41. Albert JM, Cao C, Kim KW, et al. Inhibition of poly(ADP-ribose) polymerase enhances cell death and improves tumor growth delay in irradiated lung cancer models. Clin Cancer Res 2007;13: 3033–42.
42. Liu SK, Coackley C, Krause M, Jalali F, Chan N, Bristow RG. A novel poly(ADP-ribose) polymerase inhibitor, ABT-888, radiosensitizes malignant human cell lines under hypoxia. Radiother Oncol 2008;88: 258–68.
43. Groves MD, Maor MH, Meyers C, et al. A phase II trial of high-dose bromodeoxyuridine with accelerated fractionation radiotherapy followed by procarbazine, lomustine, and vincristine for glioblastoma multiforme. Int J Radiat Oncol Biol Phys 1999;45:127–35.
44. Helleday T, Petermann E, Lundin C, Hodgson B, Sharma RA. DNA repair pathways as targets for cancer therapy. Nat Rev Cancer 2008;8:193–204.
45. Bentley J, Diggle CP, Harnden P, Knowles MA, Kiltie AE. DNA double strand break repair in human bladder cancer is error prone and involves microhomology-associated end-joining. Nucleic Acids Res 2004;32:5249–59.
46. Liu Y, Zhou K, Zhang H, et al. Polymorphisms of LIG4 and XRCC4 involved in the NHEJ pathway interact to modify risk of glioma. Hum Mutat 2008;29:381–9.
47. Greiner TC, Dasgupta C, Ho VV, et al. Mutation and genomic deletion status of ataxia telangiectasia mutated (ATM) and p53 confer specific gene expression profiles in mantle cell lymphoma. Proc Natl Acad Sci U S A 2006;103:2352–7.
48. van der Kogel AJ. Radiation-induced damage in the central nervous system: an interpretation of target cell responses. Br J Cancer Suppl 1986;7:207–17.